

Evaluation of Hydration Enthalpies of Monatomic Cations by Considering Both Long-Range and Short-Range Interactions

Nobuyuki Ichieda, Megumi Kasuno, Khaleda Banu, and Sorin Kihara*

Department of Chemistry, Kyoto Institute of Technology, Sakyo, Kyoto 606-8585, Japan

Hirohide Nakamatsu

Institute for Chemical Research, Kyoto University, Uji, Kyoto 611-0011, Japan

Received: March 31, 2003; In Final Form: June 8, 2003

The standard hydration enthalpy, $\Delta H^\circ_{\text{hyd}}$, of a monatomic cation was calculated as the sum of (1) the enthalpy due to the long-range interaction between a hydrated ion and bulk water, $\Delta H^\circ_{\text{LR}}$, (2) the enthalpy due to the short-range interaction between the ion and water molecules in the first hydration shell, $\Delta H^\circ_{\text{SR}}$, and (3) the enthalpy due to the ligand field stabilization of an ion, $\Delta H^\circ_{\text{LF}}$, which arises for a transition-metal ion. $\Delta H^\circ_{\text{LR}}$ was estimated on the basis of the Born theory assuming the radius of the hydrated ion as the interatomic distance between the ion and the oxygen atom of a water molecule in the first hydration shell, $r_{\text{M-O}}$, determined experimentally. $\Delta H^\circ_{\text{SR}}$ was evaluated on the basis of the donor–acceptor interaction between an ion and a water molecule coordinating to the ion, which was evaluated by the molecular orbital calculation of a monohydrated cluster of an ion combined with the Mulliken population analysis. $\Delta H^\circ_{\text{LF}}$ was calculated on the basis of the crystal field theory. Hydration enthalpies of 48 monatomic cations thus calculated agreed well with those observed experimentally.

1. Introduction

Since the Born equation for the evaluation of the standard solvation free energy of an ion, $\Delta G^\circ_{\text{soln}}$, was proposed,¹ various modifications of the equation have been examined to improve the accuracy of the estimation of $\Delta G^\circ_{\text{soln}}$ within the framework of the dielectric continuum model.^{2,3} The $\Delta G^\circ_{\text{soln}}$ values of many ions (especially transition-metal ions) calculated by these equations, however, do not agree with those obtained experimentally. The main reason for the disagreement is that these equations dealt with merely the electrostatic interaction between an ion and bulk water (the long-range interaction), and the short–range interaction between the ion and water molecules in the vicinity of the ion was not taken into account.^{4–6}

Several hydration models have been proposed^{7–13} on the basis of the long-range and short-range electrostatic interactions for the evaluation of the standard hydration free energy, $\Delta G^\circ_{\text{hyd}}$, or the standard hydration enthalpy, $\Delta H^\circ_{\text{hyd}}$, of an ion. However, $\Delta G^\circ_{\text{hyd}}$ and $\Delta H^\circ_{\text{hyd}}$ evaluated by these models do not agree with those determined experimentally except for those of limited kinds of ions (mainly ions of closed shells). One of the reasons for the disagreement might be that the short-range interaction in these models was evaluated on the basis of only electrostatic interactions such as charge–dipole and charge–quadrupole interactions between an ion and water molecules, but the donor–acceptor interaction between an ion and water molecules was neglected. Here, experimental^{14,15} and theoretical^{16–18} studies demonstrated the significant contribution of donor–acceptor interaction to the short-range interaction especially when the ions were transition-metal ions. Another reason might be that the ligand field stabilization in the hydration of a transition-metal ion was not considered in these models though the importance of the ligand stabilization effect has been pointed out by Holmes and McClure.¹⁹ As described above, it is not an

exaggeration to say that hydration models appropriate for the quantitative evaluation of $\Delta G^\circ_{\text{hyd}}$ or $\Delta H^\circ_{\text{hyd}}$ of a wide variety of ions have not been proposed, yet.

In the present work, a hydration model was proposed to evaluate $\Delta H^\circ_{\text{hyd}}$ of monatomic ions including alkali-metal, alkaline-earth-metal, and transition-metal ions with valences ranging from +I to +IV. In the model, not only the long-range and short-range interactions between the ion and water but also ligand field stabilization was taken into account. The evaluation of the short-range interaction was performed referring to the donor–acceptor interaction between an ion and a water molecule estimated by molecular orbital (MO) calculation of a monohydrated cluster of an ion combined with the Mulliken population analysis.

2. Theoretical Approach

2.1. Hydration Model. Since water molecules in the first hydration shell are bound strongly to the ion, these water molecules cannot be treated as a part of the bulk water, which is regarded as a dielectric continuum in the Born model. Therefore, the water phase is divided into two regions as shown in Figure 1 in the present study. One is a bulk water phase (region A), which can be regarded as a dielectric continuum with a constant relative dielectric constant, ϵ_r . The other is the region of the first hydration shell (region B).

$\Delta H^\circ_{\text{hyd}}$ was assumed to be the sum of four components: (1) the enthalpy due to the long-range interaction between the bulk water (region A) and a hydrated ion (the ion with water molecules in region B), $\Delta H^\circ_{\text{LR}}$, (2) the enthalpy due to the short-range interaction between an ion and water molecules in region B, $\Delta H^\circ_{\text{SR}}$, (3) the enthalpy due to the ligand field stabilization caused by water molecules in region B coordinating to the ion, $\Delta H^\circ_{\text{LF}}$, and (4) the enthalpy required to form a cavity to immerse an ion into water, $\Delta H^\circ_{\text{CF}}$.

$$\Delta H^\circ_{\text{hyd}} = \Delta H^\circ_{\text{LR}} + \Delta H^\circ_{\text{SR}} + \Delta H^\circ_{\text{LF}} (+ \Delta H^\circ_{\text{CF}}) \quad (1)$$

* To whom correspondence should be addressed. E-mail: kiharas@ipc.kit.ac.jp.

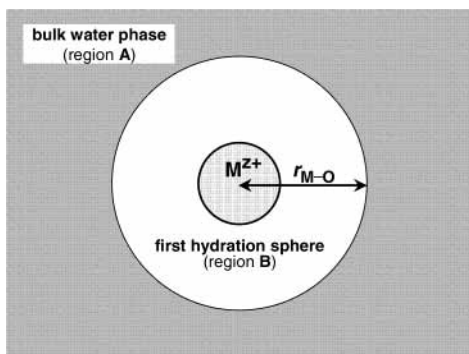


Figure 1. Schematic depiction of the hydration model of cation M^{z+} .

Since the ligand field stabilization is concerned only with the hydration of transition-metal ions, $\Delta H_{\text{LF}}^{\circ}$ was evaluated separately, distinguishing it from $\Delta H_{\text{SR}}^{\circ}$, though the ligand field stabilization is a part of the short-range interaction. $\Delta H_{\text{CF}}^{\circ}$ was neglected because the volume of a monatomic cation is small enough, and the contribution of $\Delta H_{\text{CF}}^{\circ}$ to $\Delta H_{\text{hyd}}^{\circ}$ is considered to be less than several percent of the total $\Delta H_{\text{hyd}}^{\circ}$.^{20,21}

2.1.1. Long-Range Interaction. According to the Born theory, $\Delta H_{\text{LR}}^{\circ}$ is given by

$$\Delta H_{\text{LR}}^{\circ} = (N_{\text{A}} z^2 e^2 / 8\pi\epsilon_0 r) \{ (1/\epsilon_r) + (T/\epsilon_r^2) (\partial\epsilon_r/\partial T) - 1 \} \quad (2)$$

where N_{A} , z , e , ϵ_0 , r , and T are Avogadro's number, the charge of the ion, the elementary charge, the dielectric constant of a vacuum, the ionic radius, and the absolute temperature, respectively. ϵ_r and $\partial\epsilon_r/\partial T$ are 78.39 and -0.3595 , respectively, at 25 °C.²² Since the Born equation was applied to the cation with the first hydration shell (region B) in this work, r adopted was the distance between the center of the ion and the center of the oxygen atom in the water molecule in the first hydration shell, $r_{\text{M-O}}$, which was determined experimentally (Table 1).^{17,23–37} In this connection, crystallographic ionic radii with empirical modifications were adopted as r in several types of hydration models.^{8–12} $r_{\text{M-O}}$ is considered to be preferable, however, because $r_{\text{M-O}}$ reflects a hydration structure of the ion. Though hydrogen atoms of water molecules coordinating to the ion locate outside the sphere of radius $r_{\text{M-O}}$, the discrepancy between $r_{\text{M-O}}$ and an actual radius of the hydrated ion is considered to be negligible because the O–H bond length in a water molecule is smaller than $r_{\text{M-O}}$, and the O–H bond is tilted in an aqueous solution as will be discussed later.

2.1.2. Short-Range Interaction. According to eq 1, the difference between $\Delta H_{\text{hyd}}^{\circ}$ and $\Delta H_{\text{LR}}^{\circ}$, $\Delta\Delta H^{\circ}$, is equal to the sum of $\Delta H_{\text{SR}}^{\circ}$ and $\Delta H_{\text{LF}}^{\circ}$ when the ion of interest is that of a transition metal:

$$\Delta\Delta H^{\circ} = \Delta H_{\text{SR}}^{\circ} + \Delta H_{\text{LF}}^{\circ} (\text{transition-metal ions}) \quad (3)$$

$\Delta\Delta H^{\circ}$ can be regarded as $\Delta H_{\text{SR}}^{\circ}$ when the ion is of closed shell configuration, since the ligand field stabilization does not occur ($\Delta H_{\text{LF}}^{\circ} = 0$) in this case:

$$\Delta\Delta H^{\circ} = \Delta H_{\text{SR}}^{\circ} (\text{closed shell ions}) \quad (4)$$

$\Delta\Delta H^{\circ}$ was calculated by subtracting $\Delta H_{\text{LR}}^{\circ}$ obtained on the basis of eq 2 from $\Delta H_{\text{hyd}}^{\circ}$ determined experimentally.

On the other hand, the MO calculation of a monohydrated cluster of an ion was applied to the investigation of the electronic state of the hydrated ion, and the donor–acceptor interaction between an ion and a water molecule was evaluated quantitatively. Then, a semiempirical equation for the expression of

TABLE 1: Distance between an Ion and the Oxygen Atom in a Water Molecule in the First Hydration Shell, $r_{\text{M-O}}$, Observed Experimentally^a

ion	$r_{\text{M-O}}/\text{nm}$	ref	ion	$r_{\text{M-O}}/\text{nm}$	ref
Monovalent Cations					
Li ⁺	0.206	23, 24	Rb ⁺	0.289	25
Na ⁺	0.244	23	Cs ⁺	0.307	23
K ⁺	0.281	23	Ag ⁺	0.241	23
Divalent Cations					
Be ²⁺	0.167	26	Fe ²⁺	0.216	23
Mg ²⁺	0.209	23	Co ²⁺	0.210	23
Ca ²⁺	0.240	23	Ni ²⁺	0.207	23
Sr ²⁺	0.264	23, 27	Cu ²⁺	0.210 ^b	23
Ba ²⁺	0.282	27	Zn ²⁺	0.211	23
V ²⁺	0.218	28	Cd ²⁺	0.230	23
Cr ²⁺	0.214 ^b	29, 30	Hg ²⁺	0.241	31
Mn ²⁺	0.219	23	Sn ²⁺	0.231	23
Trivalent Cations					
Al ³⁺	0.189	23	Ce ³⁺	0.255	25
Sc ³⁺	0.218	32, 33	Pr ³⁺	0.251	23,35
Ti ³⁺	0.212	28	Nd ³⁺	0.249	23
V ³⁺	0.203	28	Sm ³⁺	0.246	23
Cr ³⁺	0.198	23	Eu ³⁺	0.244	23
Mn ³⁺	0.199	17	Gd ³⁺	0.239	23
Fe ³⁺	0.202	23	Tb ³⁺	0.240	23
Ga ³⁺	0.194	17	Dy ³⁺	0.238	23
Y ³⁺	0.237	23	Er ³⁺	0.236	23
In ³⁺	0.215	34	Tm ³⁺	0.234	23
Tl ³⁺	0.223	23	Yb ³⁺	0.233	23
La ³⁺	0.253	23	Lu ³⁺	0.233	23
Tetravalent Cations					
Th ⁴⁺	0.249	36	U ⁴⁺	0.246	37

^a Mean of the reported values (at 25 °C). ^b Mean of distances in axial and equatorial positions.

$\Delta H_{\text{SR}}^{\circ}$ was proposed by comparing $\Delta\Delta H^{\circ}$ with the result of the MO calculation. Details on the MO calculation will be described in section 2.2.

2.1.3. Ligand Field Stabilization. The 3d transition-metal ion forms an octahedral aqua complex with six water molecules in an aqueous solution. Five d orbitals of the ion split into three lower orbitals, t_{2g} , and two higher orbitals, e_g , due to the ligand field of the water molecules. When d orbitals of the ion are occupied partially, ligand field stabilization occurs. On the basis of the classical crystal field theory,³⁸ $\Delta H_{\text{LF}}^{\circ}$ can be approximated as

$$\Delta H_{\text{LF}}^{\circ} = -(N_t(4Dq) + N_e(6Dq)) \quad (5)$$

where N_t and N_e are the numbers of d electrons in the e_g and t_{2g} orbitals, respectively, and the splitting parameter, Dq , is defined as 1/10 of the energy gap between the e_g and t_{2g} orbitals. The Jahn–Teller effect was not considered in this work. Ligand field stabilizations of lanthanide and actinide ions were neglected since they are negligibly small.³⁹

2.2. Molecular Orbital Calculation. The MO calculation of monohydrated clusters of alkali-metal, Ag^+ , alkaline-earth-metal, and divalent 3d transition-metal ions was carried out by the discrete variational (DV)-X α method, since an MO can be expressed as a linear combination of atomic orbitals instead of that of Gaussian or Slater functions, which has been used in other typical ab initio MO methods, and hence an accurate MO can be calculated directly by the DV-X α method. The details of the computation were described by Adachi et al.^{40,41} The spin-polarized DV-X α method was employed for calculations of transition-metal ion clusters. The exchange–correlation potential

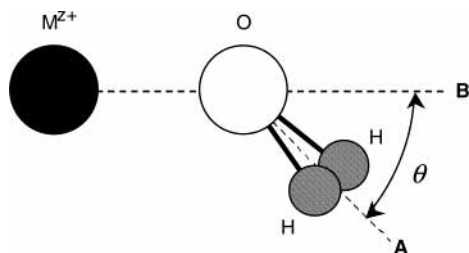


Figure 2. Geometric structure of a monohydrated cluster of cation M^{z+} .

of an electron, V_{xc} , was approximated by Slater's X α potential:

$$V_{xc} = -3\alpha(3\rho/8\pi)^{1/3} \quad (6)$$

where α and ρ are the scaling parameter and the local charge density, respectively. α in the present work was fixed to be 0.7, which was the optimal value for all molecules.⁴² The numerical atomic orbitals were obtained by solving the Schrödinger equation for each atom in the monohydrated cluster, and the orbitals were employed as basis functions as follows: $1s-\beta p$ for alkali-metal ions ($\beta = 2, 3, 4, 5,$ and 6 for Li, Na, K, Rb, and Cs ions, respectively) and alkaline-earth-metal ions ($\beta = 2, 3, 4, 5,$ and 6 for Be, Mg, Ca, Sr, and Ba ions, respectively), $1s-4p$ for all transition-metal ions, $1s$ for the hydrogen atom, and $1s-2p$ for the oxygen atom. The orbital population, $Q_i(\gamma)$, which is the number of electrons existing on an orbital γ of an atom i , the effective charge which is the total charge localizing on i , n_i , and the bond overlap population between atoms i and j , Q_{i-j} , were obtained by the Mulliken population analysis.^{43,44} Q_{i-j} is the number of electrons existing between atoms i and j , and can be regarded as a measure of the covalent character of the bond between atoms i and j . Positive and negative values of Q_{i-j} mean bonding and antibonding characters between atoms i and j , respectively.

A cluster model of a monohydrated cation, $M^{z+}\cdot H_2O$, adopted in the MO calculation is shown in Figure 2. The geometric structure of the cluster in this model was determined by taking into account the fact that the dipolar axis of the water molecule (broken line A) was found to be tilted with an angle of θ from the line connecting M^{z+} and an oxygen atom of the water molecule (broken line B) in the $M^{z+}\cdot H_2O$ cluster. This fact was observed experimentally in the analysis of the hydration structure of the ion in an aqueous solution by neutron or X-ray diffraction methods. Since θ of many metal ions observed was in the range between 30° and 60° ,^{23,45} θ was assumed to be the intermediate value, 45° , in the present work unless otherwise mentioned. The effective charge on one hydrogen atom, n_H , and the bond overlap population between the oxygen atom and one hydrogen atom, Q_{O-H} , were considered to be identical with those due to the other hydrogen atom, because the two hydrogen atoms of the water molecule were found to be located symmetrically about line A in the $M^{z+}\cdot H_2O$ cluster. The interatomic distances between M^{z+} and the oxygen atom determined experimentally for a fully hydrated ion^{17,23-37} (Table 1) were defined as r_{M-O} in $M^{z+}\cdot H_2O$ clusters unless otherwise noted. Here, the effect of hydration number on r_{M-O} is considered not to be serious. For example, Combariza and Kestner calculated the optimized structures of hydrated ions, such as $Li^+(H_2O)_n$ and $Na^+(H_2O)_n$ ($n = 1$ or 3), on the basis of density functional theory and reported that the difference between r_{M-O} in the monohydrated ion cluster and that in the trihydrated cluster was not very large and was about 2%.⁴⁶ The O-H bond length and H-O-H angle in the water molecule in $M^{z+}\cdot H_2O$ clusters were taken as 96

TABLE 2: Hydration Enthalpies Reported as Experimental Values, $-\Delta H_{\text{hyd}}^\circ$ (exptl), and Contributions of Long-Range, $-\Delta H_{\text{LR}}^\circ$, Short-Range, $-\Delta H_{\text{SR}}^\circ$, and Ligand Field, $-\Delta H_{\text{LF}}^\circ$, Interactions to Hydration Enthalpies of Monatomic Metal Ions Evaluated in the Present Work

ion	$-\Delta H_{\text{hyd}}^\circ$ (exptl) ^{a/} kJ mol ⁻¹	$-\Delta H_{\text{LR}}^\circ$ ^{b/} kJ mol ⁻¹	$-\Delta H_{\text{SR}}^\circ$ ^{c/} kJ mol ⁻¹	$-\Delta H_{\text{LF}}^\circ$ ^{d/} kJ mol ⁻¹	$-\Delta H_{\text{hyd}}^\circ$ (calcd) ^{e/} kJ mol ⁻¹
Monovalent Cations					
Li ⁺	531	339	185	0	524
Na ⁺	416	286	119	0	405
K ⁺	334	248	72	0	321
Rb ⁺	308	241	64	0	305
Cs ⁺	283	227	46	0	273
Ag ⁺	483	290	124	0	413
Divalent Cations					
Be ²⁺	2510	1671	806	0	2477
Mg ²⁺	1949	1335	596	0	1931
Ca ²⁺	1602	1163	488	0	1651
Sr ²⁺	1470	1057	422	0	1479
Ba ²⁺	1332	990	380	0	1370
V ²⁺	1629	1280	562	169	2011
Cr ²⁺	1933	1304	577	100	1981
Mn ²⁺	1874	1274	558	0	1832
Fe ²⁺	1972	1292	569	48	1909
Co ²⁺	2036	1329	592	96	2017
Ni ²⁺	2119	1348	604	123	2075
Cu ²⁺	2123	1329	592	93	2014
Zn ²⁺	2070	1323	588	0	1911
Cd ²⁺	1833	1213	520	0	1733
Hg ²⁺	1853	1158	485	0	1643
Sn ²⁺	1577	1208	517	0	1725
Trivalent Cations					
Al ³⁺	4715	3322	1145	0	4467
Sc ³⁺	3967	2880	961	0	3842
Ti ³⁺	4340	2962	995	97	4054
V ³⁺	4450	3093	1050	172	4315
Cr ³⁺	4670	3171	1082	253	4507
Mn ³⁺	4640	3155	1076	151	4381
Fe ³⁺	4462	3109	1056	0	4165
Ga ³⁺	4309	3237	1109	0	4346
Y ³⁺	3594	2649	865	0	3515
In ³⁺	4127	2921	978	0	3898
Tl ³⁺	4125	2816	934	0	3750
La ³⁺	3312	2482	795	0	3277
Ce ³⁺	3367	2462	787	0	3250
Pr ³⁺	3411	2502	804	0	3305
Nd ³⁺	3447	2522	812	0	3334
Sm ³⁺	3492	2553	825	0	3377
Eu ³⁺	3535	2573	833	0	3407
Gd ³⁺	3549	2627	856	0	3483
Tb ³⁺	3580	2616	851	0	3468
Dy ³⁺	3604	2638	860	0	3499
Er ³⁺	3674	2661	870	0	3530
Tm ³⁺	3695	2683	879	0	3563
Yb ³⁺	3742	2695	884	0	3579
Lu ³⁺	3695	2695	884	0	3579
Tetravalent Cations					
Th ⁴⁺	6057	4483	1162	0	5645
U ⁴⁺	6572	4538	1179	0	5717

^a Standard hydration enthalpy reported as the experimental value.⁴⁸

^b Enthalpy due to the long-range interaction calculated by eq 2.

^c Enthalpy due to the short-range interaction calculated by eq 7.

^d Enthalpy due to the ligand field stabilization calculated by eq 5. ^e Total hydration enthalpy calculated by eq 1.

pm and 104° , respectively.⁴⁷ Since the structure of the hydrated cluster adopted in the MO calculation was that determined experimentally as mentioned above, further optimization of the configuration (bond lengths and bond angles) based on the minimization of the total energy of electrons in the system was not performed in the calculation.

3. Results and Discussion

3.1. Long-Range Interaction. The $\Delta H_{\text{LR}}^\circ$ values of 48 monatomic cations were calculated by substituting r_{M-O} for r in eq 2 as listed in Table 2. The $\Delta H_{\text{LR}}^\circ$ values were 60–80%

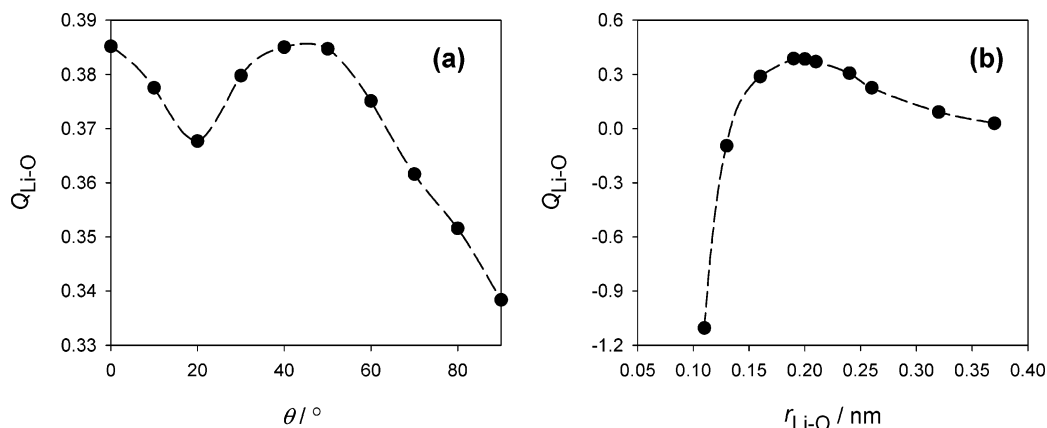


Figure 3. Relation between (a) the tilt angle, θ , or (b) the Li–O distance, $r_{\text{Li-O}}$, and the overlap population between Li^+ and O, $Q_{\text{Li-O}}$.

TABLE 3: Orbital Populations on Orbitals γ , $Q(\gamma)$, and Effective Charges, n , on Li, O, and H in the $\text{Li}^+\cdot\text{H}_2\text{O}$ Cluster

	Li	O	H ^a
$Q(1s)$	2.00	2.00	0.71
$Q(2s)$	0.09	1.66	
$Q(2p)$	0.18	4.63	
n	+0.73	-0.30	+0.28

^a Values for the two H atoms in a water molecule are identical.

of $\Delta H_{\text{hyd}}^\circ$ observed experimentally, $\Delta H_{\text{hyd}}^\circ(\text{exptl})$,⁴⁸ and hence 20–40% of $\Delta H_{\text{hyd}}^\circ$ was considered to be attributable to the short-range interaction and the ligand field stabilization.

3.2. Short-Range Interaction. *3.2.1. Donor–Acceptor Interaction between Li^+ and a Water Molecule.* The donor–acceptor interaction between M^{z+} and a water molecule was examined in detail, adopting Li^+ as an example of M^{z+} . Table 3 lists the orbital population and n on Li, O, and H in the $\text{Li}^+\cdot\text{H}_2\text{O}$ cluster obtained by the MO calculation combined with the Mulliken population analysis. The $r_{\text{M-O}}$ and θ assumed in the calculation were 0.206 nm and 45° , respectively.

The result of the calculation indicates the following facts: (1) The water molecule in the cluster is polarized due to the electric field caused by Li^+ in addition to the difference in electronegativity between oxygen and hydrogen atoms. Two hydrogen atoms and one oxygen atom in the cluster are charged positively ($n_{\text{H}} = +0.28$) and negatively ($n_{\text{O}} = -0.30$), respectively. (2) The positive charge of 0.26 ($= 2n_{\text{H}} + n_{\text{O}}$) is localized on the H_2O moiety, and the corresponding negative charge of 0.26 is transferred from H_2O to unoccupied 2s and 2p orbitals of Li^+ , where the water molecule acts as a donor. Consequently, n_{Li} is reduced from +1, which is the charge of a monovalent cation in the isolated state, to +0.73. (3) A single bond is formed between the oxygen and hydrogen atoms, and $Q_{\text{O-H}}$ is 0.653. $Q_{\text{Li-O}}$ is 0.385, which is considerably large compared to $Q_{\text{O-H}}$. This result indicates that the short-range interaction between Li^+ and the oxygen atom involves a significant covalent character.

To clarify the effect of θ on $Q_{\text{Li-O}}$, the MO calculation of the $\text{Li}^+\cdot\text{H}_2\text{O}$ cluster with various θ values from 0° to 90° was performed (Figure 3a). $r_{\text{Li-O}}$ was fixed at 0.206 nm in the calculation. Two maximums of $Q_{\text{Li-O}}$ appearing at 0° and around 45° can be understood by considering the orientation of two lone pairs of electrons of a water molecule. One of the lone pairs is directed to the ion at $\theta = 45^\circ$, and the orbitals of the lone pair overlap with empty 2s and 2p orbitals of Li^+ . When θ is 0° , Li^+ locates between two lone pairs, and both lone pairs contribute to the covalent bond between Li^+ and O. However, the former orientation is preferred in the aqueous solution.^{23,45}

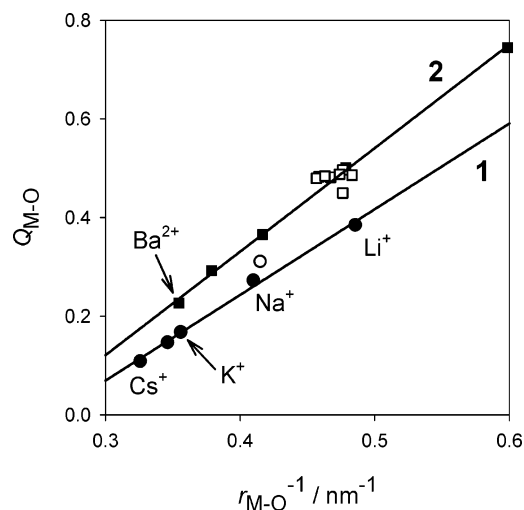


Figure 4. Dependence of the overlap population between M^{z+} and O, $Q_{\text{M-O}}$, on the ionic radius of M^{z+} , $r_{\text{M-O}}$: ●, alkali-metal ions; ○, Ag^+ ; ■, alkaline-earth-metal ions; □, divalent transition-metal ions; solid lines, determined by the least-squares method using $Q_{\text{M-O}}$ for alkali-metal (line 1) and alkaline-earth-metal (line 2) ions.

The effect of $r_{\text{Li-O}}$ on $Q_{\text{Li-O}}$ was also examined as shown in Figure 3b. θ was fixed at 45° in the calculation. When $r_{\text{Li-O}}$ is less than 0.2 nm, $Q_{\text{Li-O}}$ decreases with decreasing $r_{\text{Li-O}}$. When Li^+ and a water molecule are very close ($r_{\text{Li-O}} < 0.13$ nm), $Q_{\text{Li-O}}$ is negative, which implies the repulsive interaction between Li^+ and a water molecule. The maximum covalent character is obtained when $r_{\text{Li-O}}$ is about 0.2 nm, which agrees with $r_{\text{Li-O}}$ observed experimentally (0.206 nm).

These results suggest the considerable contribution of the covalent character between Li^+ and a water molecule in the determination of the hydration structure in region B though other interactions such as charge–dipole and charge–quadrupole interactions also affect the hydration structure.

3.2.2. Donor–Acceptor Interaction between M^{z+} and a Water Molecule. The donor–acceptor interaction between M^{z+} and a water molecule ($\text{M}^{z+} = \text{alkali-metal ions, Ag}^+, \text{alkaline-earth-metal ions, and divalent 3d transition-metal ions}$) was investigated with the aid of the MO calculation (see the results of the calculation in Table 1S in the Supporting Information).

$Q_{\text{M-O}}$ obtained by the MO calculation is plotted as a function of $r_{\text{M-O}}^{-1}$ in Figure 4. The $Q_{\text{M-O}}$ values in all $\text{M}^{z+}\cdot\text{H}_2\text{O}$ clusters were positive, and linear relationships with slopes of 1.7 and 2.1 nm were found in the relation between $Q_{\text{M-O}}$ and $r_{\text{M-O}}^{-1}$ for monovalent ions and divalent ions including transition-metal ions, respectively. $Q_{\text{M-O}}$ increased with decreasing $r_{\text{M-O}}$. For

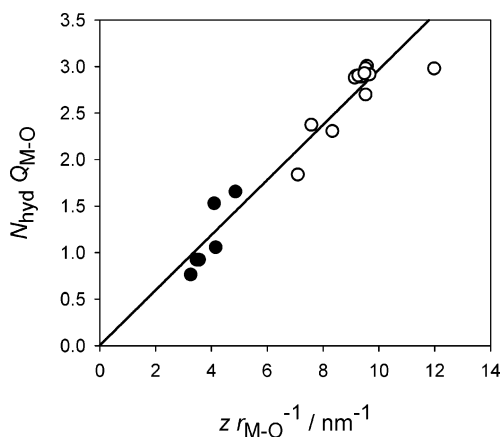


Figure 5. Dependence of $N_{\text{hyd}}Q_{\text{M-O}}$ on $z/r_{\text{M-O}}$ (N_{hyd} = the hydration number obtained experimentally, $Q_{\text{M-O}}$ = the overlap population between $\text{M}^{\text{z+}}$ and O, z = the charge of $\text{M}^{\text{z+}}$, and $r_{\text{M-O}}$ = the ionic radius of $\text{M}^{\text{z+}}$: ●, monovalent ions; ○, divalent ions; solid line, determined by the least-squares method using the data on all ions.

example, $Q_{\text{Li-O}}$ ($r_{\text{Li-O}} = 0.206$) is about 4 times larger than $Q_{\text{Cs-O}}$ ($r_{\text{Cs-O}} = 0.307$), in agreement with the covalent character in the hydration of an alkali-metal ion estimated on the basis of the successive hydration enthalpy of the ion in the gas phase by Džidić and Kebarle.¹⁴ Since the $r_{\text{M-O}}$ values of divalent transition-metal ions studied were identical (about 0.21 nm) with each other, the $Q_{\text{M-O}}$ values of these ions are about the same. However, even though $r_{\text{M-O}}$ of K^+ (0.281 nm) is similar to that of Ba^{2+} (0.282 nm), $Q_{\text{Ba-O}}$ is about 1.4 times larger than $Q_{\text{K-O}}$. The $Q_{\text{M-O}}$ of a divalent ion is larger than that of a monovalent ion when $r_{\text{M-O}}$ values of the ions are the same. As seen in Figure 4, the high covalent nature also exists between Ag^+ and a water molecule. The $Q_{\text{M-O}}$ for the Ag^+ cluster is 14% larger than that for the Na^+ cluster, though $r_{\text{Ag-O}}$ is identical with $r_{\text{Na-O}}$.

3.2.3. Effect of Hydration Number. Although $Q_{\text{M-O}}$ in the bond between an ion and one water molecule was evaluated on the basis of the MO calculation of a monohydrated cluster in previous sections as the measure of the covalent character of the bond between an ion and water molecules in the first hydration shell (region B in Figure 1), an ion is coordinated by plural water molecules in an actual aqueous solution. Therefore, the number of water molecules in the first hydration shell (i.e., hydration number, N_{hyd}) should be taken into account in the estimation of $\Delta H^{\circ}_{\text{SR}}$. The contribution of the covalent character between an ion and all water molecules in the first hydration

shell was assumed to be approximated by $N_{\text{hyd}}Q_{\text{M-O}}$ in the present work. This simple approximation was supported by the result that the $N_{\text{hyd}}Q_{\text{M-O}}$ values of both monovalent and divalent ions calculated were proportional to $z/r_{\text{M-O}}$ as shown in Figure 5. Here, N_{hyd} determined experimentally²³ by the neutron or X-ray diffraction method was used in the calculation of $N_{\text{hyd}}Q_{\text{M-O}}$ (cf. Table 1S in the Supporting Information).

3.2.4. Evaluation of $\Delta H^{\circ}_{\text{SR}}$. The $\Delta\Delta H^{\circ}$ values for 19 ions, on which the MO calculation was done, are plotted as a function of $N_{\text{hyd}}Q_{\text{M-O}}$ in Figure 6a. The $\Delta\Delta H^{\circ}$ of closed shell ions, i.e., $\Delta H^{\circ}_{\text{SR}}$ (see, eq 4), is linear to $N_{\text{hyd}}Q_{\text{M-O}}$ even though the short-range interaction between an ion and water molecules is considered to consist of plural interactions such as donor-acceptor, charge-dipole, and charge-quadrupole interactions. Since $N_{\text{hyd}}Q_{\text{M-O}}$ is proportional to $z/r_{\text{M-O}}$ as mentioned previously, $\Delta H^{\circ}_{\text{SR}}$ is expected to be linear to $z/r_{\text{M-O}}$.

Figure 6b shows the relation between $\Delta\Delta H^{\circ}$ and $z/r_{\text{M-O}}$. The least-squares method was applied to the $\Delta\Delta H^{\circ}$ of alkali-metal and alkaline-earth-metal ions ("training" set of 10 ions, Li^+ , Na^+ , K^+ , Rb^+ , Cs^+ , Be^{2+} , Mg^{2+} , Ca^{2+} , Sr^{2+} , and Ba^{2+}), and $\Delta\Delta H^{\circ}$, which can be regarded as $\Delta H^{\circ}_{\text{SR}}$ (see eq 4), was found to be approximated by

$$\Delta H^{\circ}_{\text{SR}} = -87.1(z/r_{\text{M-O}}) + 237.5 \quad (7)$$

where $\Delta H^{\circ}_{\text{SR}}$ and $r_{\text{M-O}}$ are expressed in kilojoules per mole and nanometers, respectively. Here, the regression coefficient was 0.99. The deviations of $\Delta\Delta H^{\circ}$ for transition-metal ions from the linear regression line are attributable to the ligand field stabilization effect. Although Ag^+ has a closed shell configuration, the absolute value of $\Delta H^{\circ}_{\text{SR}}$ of Ag^+ is larger than that expected from eq 7 by using $r_{\text{Ag-O}}$ observed experimentally. This result is attributable to the strong covalent interaction between Ag^+ and a water molecule as described in section 3.2.2.

3.3. Ligand Field Stabilization. The $\Delta H^{\circ}_{\text{LF}}$ values calculated according to eq 5 are listed in Table 2 (cf. the details of the calculation of $\Delta H^{\circ}_{\text{LF}}$ given in Table 2S in the Supporting Information). The Dq values determined experimentally on the basis of absorption spectra³⁸ were used in the calculation. The absolute value of $\Delta\Delta H^{\circ}$ of V^{2+} is smaller than $\Delta H^{\circ}_{\text{SR}}$ calculated by eq 7 (Figure 6b), which implies negative ligand field stabilization (see eq 3), though the stabilization is expected to be large from the fact that the absolute value of the $\Delta H^{\circ}_{\text{LF}}$ of V^{2+} is the largest among those of divalent 3d transition-metal ions.³⁸ The reason for this conflict will be discussed later.

3.4. Comparison of $\Delta H^{\circ}_{\text{hyd}}$ Calculated with $\Delta H^{\circ}_{\text{hyd}}$ Determined Experimentally. The $\Delta H^{\circ}_{\text{hyd}}$ values of 48 monatomic

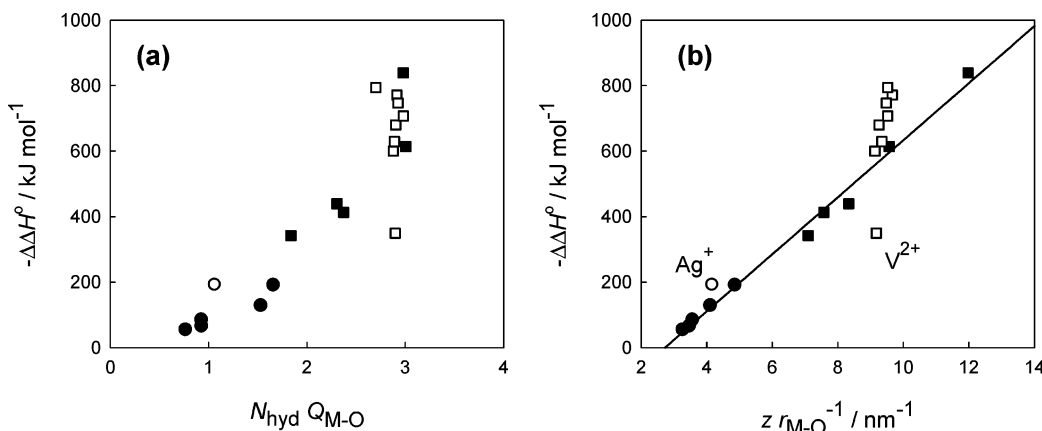


Figure 6. Dependence of the difference between the hydration enthalpy observed experimentally and that due to the long-range interaction calculated on the basis of the Born equation, $\Delta\Delta H^{\circ}$, on (a) $N_{\text{hyd}}Q_{\text{M-O}}$ and (b) $z/r_{\text{M-O}}$: ●, alkali-metal ions; ○, Ag^+ ; ■, alkaline-earth metals; □, divalent transition-metal ions; solid line, determined by the least-squares method using $\Delta\Delta H^{\circ}$ for alkali-metal and alkaline-earth-metal ions.

TABLE 4: Bond Overlap Populations between X⁻ and H(1),^a Q_{X-H(1)}, and Effective Charges, n, on X⁻, O, H(1), and H(2)^b Obtained by the MO Calculation of a Monohydrated Halide Ion Cluster, X⁻·H₂O

ion	Q _{X-H(1)}	n _X	n _{H(1)}	n _O	n _{H(2)}
F ⁻	-0.135	-0.84	+0.38	-0.87	+0.33
Cl ⁻	-0.268	-0.81	+0.30	-0.82	+0.33
Br ⁻	-0.041	-0.86	+0.34	-0.82	+0.33
I ⁻	+0.039	-0.89	+0.36	-0.80	+0.33

^a One of the two hydrogen atoms in H₂O coordinated to X⁻. ^b The other hydrogen atom in H₂O.

cations (“training” set of 10 ions and “test” set of 38 ions) with valences ranging from +I to +IV were estimated as the sum of $\Delta H^{\circ}_{\text{LR}}$, $\Delta H^{\circ}_{\text{SR}}$, and $\Delta H^{\circ}_{\text{LF}}$ calculated by eqs 2, 7, and 5, respectively (Table 2). $\Delta H^{\circ}_{\text{hyd}}$ thus calculated, $\Delta H^{\circ}_{\text{hyd}}(\text{calcd})$, agreed well with $\Delta H^{\circ}_{\text{hyd}}(\text{exptl})$. Deviations of $\Delta H^{\circ}_{\text{hyd}}(\text{calcd})$ from $\Delta H^{\circ}_{\text{hyd}}(\text{exptl})$ were within 5% for 23 ions in the test set and within 5–10% for 11 ions in the test set. However, deviations for Ag⁺, V²⁺, Hg²⁺, and U⁴⁺ were more than 10%. The large deviation of $\Delta H^{\circ}_{\text{hyd}}(\text{calcd})$ for Ag⁺ might be attributable to the strong covalent bond between Ag⁺ and water molecules (see section 3.2.2), but those for Hg²⁺ and U⁴⁺ are not clear at the moment. The $\Delta H^{\circ}_{\text{hyd}}(\text{exptl})$ for V²⁺ adopted in this work, -1629 kJ mol⁻¹, which was reported by Marcus,⁴⁸ was about 300 kJ mol⁻¹ larger than those for other divalent transition-metal ions, and also much larger than $\Delta H^{\circ}_{\text{hyd}}(\text{calcd})$. However, when the $\Delta H^{\circ}_{\text{hyd}}(\text{exptl})$ of V²⁺ reported by Smith⁴⁹ (-1918 kJ mol⁻¹) was adopted, $\Delta H^{\circ}_{\text{hyd}}(\text{exptl})$ agreed with $\Delta H^{\circ}_{\text{hyd}}(\text{calcd})$ with a deviation of 5%. Therefore, the negative ligand field stabilization estimated for V²⁺ in the previous section might be due to the adoption of too large a $\Delta H^{\circ}_{\text{hyd}}(\text{exptl})$ reported by Marcus.⁴⁸

3.5. Donor–Acceptor Interaction between a Halide Ion and a Water Molecule. The MO calculation of X⁻·H₂O (X⁻ = F⁻, Cl⁻, Br⁻, and I⁻) clusters was also performed. The cluster was considered to consist of X⁻ to which a H₂O coordinated through the bonding between X⁻ and a hydrogen atom of H₂O, H(1), in the first hydration shell.²³ The X⁻, H(1), and O of the H₂O were assumed to be aligned on a straight line in the calculation, because the H(1)–X–O angle was reported to be less than 10° in aqueous solutions on the basis of neutron diffraction analysis.^{23,45} The interatomic distance between F⁻, Cl⁻, Br⁻, or I⁻ and O in the X⁻·H₂O cluster used was that between the center of X⁻ and the O of the water molecule in the first hydration shell determined experimentally,²³ and was 0.264, 0.317, 0.332, or 0.363, respectively. The Q_{X-H(1)} and n on X⁻, O, H(1), and another hydrogen atom in H₂O, H(2), obtained by MO calculation are tabulated in Table 4. Negative charges were transferred from X⁻ to H₂O in X⁻·H₂O clusters, and H₂O behaved as an acceptor in X⁻·H₂O clusters. The amount of charge transferred from X⁻ to H₂O was in the range from 0.11 to 0.19, and almost independent of the kind of X⁻. Negative Q_{X-H(1)} values in clusters of F⁻, Cl⁻, and Br⁻ are attributable to the repulsive interaction between X⁻ and H₂O. (Though Q_{X-H(1)} for I⁻ is positive, it is much smaller than Q_{M-O} in M^{z+}·H₂O clusters.) Therefore, it can be concluded that the covalent character in the donor–acceptor interaction between X⁻ and H₂O is negligible, which is in contrast to the case of M^{z+}·H₂O clusters.

4. Conclusion

In the evaluation of $\Delta H^{\circ}_{\text{hyd}}$ in the present work, the contribution of $\Delta H^{\circ}_{\text{CF}}$ to $\Delta H^{\circ}_{\text{hyd}}$ was neglected, and $\Delta H^{\circ}_{\text{SR}}$ was formulated by a function of a simple term, $z/r_{\text{M-O}}$, on the basis

of the relation observed empirically between $\Delta H^{\circ}_{\text{SR}}$ and $z/r_{\text{M-O}}$ for 10 closed shell ions, which was not a sufficiently large number of ions. Nevertheless, $\Delta H^{\circ}_{\text{hyd}}(\text{calcd})$ agreed well with $\Delta H^{\circ}_{\text{hyd}}(\text{exptl})$, indicating that it is useful to estimate $\Delta H^{\circ}_{\text{hyd}}$ in the combination of the long-range interaction, short-range interaction, and ligand field stabilization.

Though the short-range interaction between an ion and water is considered to be composed of plural interactions such as donor–acceptor, charge–dipole, and charge–quadrupole interactions, $\Delta H^{\circ}_{\text{SR}}$ was found to be linear to the product of N_{hyd} and Q_{M-O} estimated by DV-X α MO calculation combined with the Mulliken population analysis. $\Delta H^{\circ}_{\text{SR}}$ was also found to be well fitted by the simple function of $z/r_{\text{M-O}}$ (eq 7), when $r_{\text{M-O}}$ was taken as the distance between the center of the ion and the center of the oxygen atom in the water molecule in the first hydration shell. Although the physicochemical meaning of eq 7 has not been clarified yet, the model proposed in this work has been proved to be useful for the evaluation $\Delta H^{\circ}_{\text{hyd}}$ of a large variety of ions compared with the model adopted in conventional modified Born equations^{2,3} or the semicontinuum model^{50–52} for MO calculations.

Acknowledgment. This work was supported by Grants-in-Aid for Scientific Research (Nos. 751, 13129204, and 13554031) from the Ministry of Education, Culture, Sports, Science and Technology, Japan.

Supporting Information Available: Table 1S, bond overlap population, Q_{M-O}, between M^{z+} and O, effective charges, n, on M^{z+}, O, and H obtained by the MO calculations of monohydrated cation clusters, M^{z+}·H₂O, and hydration number of M^{z+}, N_{hyd}, obtained experimentally, and Table 2S, calculation of the enthalpy due to the ligand field stabilization, $\Delta H^{\circ}_{\text{LF}}$. This material is available free of charge via the Internet at <http://pubs.acs.org>.

References and Notes

- Born, M. Z. *Phys.* **1920**, *1*, 45–48.
- Liszi, J.; Ruff, I. In *The Chemical Physics of solvation Part A Theory of Solvation*; Dogonadze, R. R., Kálman, E., Kornyshev, A. A., Ulstrup, J., Eds.; Elsevier: Amsterdam, 1985; Chapter 4.
- Bockris, J. O.; Reddy, A. K. N. *Modern Electrochemistry 1: Ionics*, 2nd ed.; Plenum: New York, 1998.
- Chan, D. Y. C.; Mitchell, D. J.; Ninham, B. W. *J. Chem. Phys.* **1979**, *70*, 2946–2957.
- Hirata, F.; Redfern, P.; Levy, R. M. *Int. J. Quantum Chem.* **1988**, *15*, 179–190.
- Babu, C. S.; Lim, C. J. *Chem. Phys. B* **1999**, *103*, 7958–7968.
- Bernal, J. D.; Fowler, R. H. *J. Chem. Phys.* **1933**, *1*, 515–548.
- Eley, D. D.; Evans, M. G. *Trans. Faraday Soc.* **1938**, *34*, 1093–1112.
- Buckingham, A. D. *Discuss. Faraday Soc.* **1957**, *24*, 151–157.
- Muirhead-Gould, J. S.; Laider, K. J. *Trans. Faraday Soc.* **1967**, *63*, 944–952.
- Goldman, S.; Bates, R. G. *J. Am. Chem. Soc.* **1972**, *94*, 1476–1484.
- Bockris, J. O'M.; Saluja, P. P. S. *J. Phys. Chem.* **1972**, *76*, 2298–2310.
- Miyakawa, K.; Kaizu, Y.; Kobayashi, H. *J. Chem. Soc., Faraday Trans.* **1988**, *84*, 1517–1529.
- Džidić, I.; Kebarle, P. *J. Phys. Chem.* **1970**, *74*, 1466–1474.
- Mayer, U.; Gutmann, V. *Struct. Bonding* **1972**, *12*, 113–140.
- Blum, L.; Fawcett, W. R. *J. Phys. Chem.* **1992**, *96*, 408–414.
- Åkesson, R.; Pettersson, L. G. M.; Sandström, M.; Wahlgren, U. *J. Am. Chem. Soc.* **1994**, *116*, 8691–8704.
- Kallies, B.; Meier, R. *Inorg. Chem.* **2001**, *40*, 3101–3112.
- Holmes, O. G.; McClure, D. S. *J. Chem. Phys.* **1957**, *26*, 1686–1694.
- Izutsu, K. *Electrochemistry in Nonaqueous Solutions*; Wiley-VCH: Weinheim, Germany, 2002; Chapter 2.2.
- Lahiri, S. C. Z. *Phys. Chem.* **2000**, *214*, 27–44.
- Marcus Y. *Biophys. Chem.* **1994**, *51*, 111–127.

- (23) Ohtaki, H.; Radnai, T. *Chem. Rev.* **1993**, *93*, 1157–1204.
- (24) Yamagami, M.; Yamaguchi, T.; Wakita, H. *J. Chem. Phys.* **1994**, *100*, 3122–3126.
- (25) Marcus, Y. *Chem. Rev.* **1988**, *88*, 1475–1498.
- (26) Yamaguchi, T.; Ohtaki, H.; Spohr, E.; Pálinkás, G.; Heinzinger, K.; Probst, M. M. *Z. Naturforsch.* **1986**, *41a*, 1175–1185.
- (27) Persson, I.; Sandström, M.; Yokoyama, H. *Z. Naturforsch.* **1995**, *50a*, 21–37.
- (28) Miyanaga, T.; Watanabe, I.; Ikeda, S. *Bull. Chem. Soc. Jpn.* **1990**, *63*, 3282–3287.
- (29) Ikeda, S.; Watanabe, I.; Miyanaga, T. In *Structure and Dynamics of Solutions*; Ohtaki, H., Yamatera, H., Eds.; Elsevier Science: New York, 1992; pp 39–56.
- (30) Sham, T. K.; Hastings, J. B.; Perlman, M. L. *Chem. Phys. Lett.* **1981**, *83*, 391–396.
- (31) Sandström, M.; Persson, I.; Åhrland, S. *Acta Chem. Scand.* **1978**, *A32*, 607–625.
- (32) Kanno, H.; Yamaguchi, T.; Ohtaki, H. *J. Phys. Chem.* **1989**, *93*, 1695–1697.
- (33) Ohtaki, H.; Fukushima, N.; Yamaguchi, T. In *Structure and Dynamics of Solutions*; Ohtaki, H., Yamatera, H., Eds.; Elsevier Science: New York, 1992; pp 24–39.
- (34) Maeda, M.; Ohtaki, H. *Bull. Chem. Soc. Jpn.* **1977**, *50*, 1893–1894.
- (35) Habenschuss, A.; Spedding, F. H. *J. Chem. Phys.* **1979**, *70*, 3758–3763.
- (36) Johansson, G.; Magini, M.; Ohtaki, H. *J. Solution Chem.* **1991**, *20*, 775–792.
- (37) Pocev, S.; Johansson, G. *Acta Chem. Scand.* **1973**, *27*, 2146–2160.
- (38) Dunn, T. M.; McClure, D. S.; Pearson, R. G. *Some Aspects of Crystal Field Theory*; Harper & Row: New York, 1965; Chapter 4.
- (39) Huheey, J. E. *Inorganic Chemistry*, 4th ed.; Harper & Row: New York, 1993; Chapter 16.
- (40) Adachi, H.; Tsukada, M.; Satoko, C. *J. Phys. Soc. Jpn.* **1978**, *45*, 875–883.
- (41) Adachi, H.; Shiokawa, S.; Tsukada, M.; Satoko, C.; Sugano, S. *J. Phys. Soc. Jpn.* **1979**, *47*, 1528–1537.
- (42) Baerends, E. J.; Ros, P. *Chem. Phys.* **1973**, *2*, 52–59.
- (43) Mulliken, R. S. *J. Chem. Phys.* **1955**, *23*, 1833–1840.
- (44) Mulliken, R. S. *J. Chem. Phys.* **1955**, *23*, 1841–1946.
- (45) Marcus, Y. *Ion solvation*; Wiley & Sons: New York, 1985; Chapter 5.
- (46) Combariza, J. E.; Kestner, N. R. *J. Phys. Chem.* **1995**, *99*, 2717–2723.
- (47) Kern, C. W.; Karplus, M. The water molecule. In *Water A comprehensive treatise*; Franks, F., Ed.; Plenum Press: New York, 1972; Vol. 1, pp 21–91.
- (48) Marcus, Y. *Ion Properties*; Marcel Dekker: New York, 1997; Chapter 8.
- (49) Smith, D. W. *J. Chem. Educ.* **1977**, *54*, 540–542.
- (50) Cramer, C. J.; Truhlar, D. G. *Chem. Rev.* **1999**, *99*, 2161–2200.
- (51) Pliego, J. R., Jr.; Riveros, J. M. *J. Phys. Chem. A* **2001**, *105*, 7241–7247.
- (52) Martínez, J. M.; Pappalardo, R. R.; Marcos, E. S.; Mennucci, B.; Tomasi, J.; *J. Phys. Chem. B* **2002**, *106*, 1118–1123.